J Wood Sci (2002) 48:132–137

ORIGINAL ARTICLE

Laurence R. Schimleck · Robert Evans
A. Colin Matheson

Estimation of *Pinus radiata* D. Don clear wood properties by near-infrared spectroscopy

Received: January 12, 2001 / Accepted: May 2, 2001

Abstract The use of calibrated near-infrared (NIR) spectroscopy for predicting of a range of solid wood properties is described. The methods developed are applicable to large-scale nondestructive forest resource assessment and to tree breeding and silviculture programs. A series of *Pinus radiata* D. Don (radiata pine) samples were characterized in terms of density, longitudinal modulus of elasticity (E_L), and microfibril angle (MFA). NIR spectra were obtained from the radial/longitudinal face of each sample and used to generate calibrations for the measured physical properties. The relations between laboratory-determined data and NIR fitted data were good in all cases, with coefficients of determination (R^2) ranging from 0.68 for 100/MFA to 0.94 for density$_{strip}$. A good relation (R^2 = 0.83) was also obtained for E_L estimated using data collected by SilviScan-2. The finding suggests that an NIR instrument could be calibrated to estimate the E_L of increment cores based on SilviScan data. In view of the rapidly expanding range of applications for this technique, it is concluded that appropriately calibrated NIR spectroscopy could form the basis of a testing instrument capable of predicting a range of properties from a single spectrum obtained from the product or from the raw material.

Key words Near-infrared spectroscopy · *Pinus radiata* D. Don · Solid wood properties

L.R. Schimleck (✉) · R. Evans
CSIRO Forestry and Forest Products, Private Bag 10, Clayton South MDC, Victoria, 3169 Australia
Tel. +61-3-9545-2142; Fax +61-3-9545-2448
e-mail: l.schimleck@ffp.csiro.au

A.C. Matheson
CSIRO Forestry and Forest Products, PO Box E4008, Kingston, ACT, 2604 Australia

Introduction

Rapid cost-effective methods for measuring wood quality are extremely important to tree improvement programs where it is necessary to test large numbers of trees. Traditional methods of assessing wood quality have involved felling selected trees, which is time-consuming, labor-intensive, and destructive. A nondestructive option is to sample trees using increment cores. Wood quality parameters, such as density and microfibril angle (MFA), can be measured rapidly on SilviScan-1[1] and SilviScan-2,[2,3] which have been specifically designed to test increment cores using a combination of scanning X-ray microdensitometry, X-ray diffractometry, and image analysis.

An important wood quality parameter is wood stiffness (longitudinal modulus of elasticity, or E_L). In a recent study, based on a set of 104 *Eucalyptus delegatensis* R.T. Baker (alpine ash) samples, Evans and Ilic[4] demonstrated that E_L can be rapidly predicted from measurements of density and MFA. The stiffness of these samples had been measured using a rapid sonic technique and a conventional static technique.[5]

These samples were later examined by Schimleck et al.,[6] who obtained near-infrared (NIR) spectra from the radial/longitudinal face of each sample. The NIR spectra were used to generate calibrations for a number of physical properties measured by Evans and Ilic[4] and Ilic.[5] Schimleck et al.[6] obtained good relations for all properties, with coefficients of determination (R^2) ranging from 0.77 for the modulus of rupture (MOR) through 0.90 for E_L to 0.93 for density. Schimleck et al.[6] concluded that NIR spectroscopy had the potential to predict a range of solid wood properties in *E. delegatensis*.

The work reported by Schimleck et al.[6] was for a hardwood species. The aim of our study was to apply the methods to a softwood species. NIR spectroscopy was used to estimate density, MFA, and E_L of a series of 104 *Pinus radiata* D. Don samples. The samples were well characterized, having been the subject of previous research.[7]

Experimental

Sample preparation

Dried clear wood samples of mature *P. radiata* trees from Tallaganda, Canberra, Australia were used in this study. The trees were planted in 1971 and harvested in 1994 at age 23. Boards were cut from green logs, kiln-dried, planed to 90 × 35 mm transversely and then stress-graded. Samples (approximately 300 mm long) with a range of stress grades were then removed from the boards. A small strip (2 mm tangentially, 7 mm longitudinally, ~20 mm radially) was cut from one end of each sample for MFA analysis by SilviScan-2 and NIR, as described below.

Wood properties

Dimensions and masses of the dried 300-mm clear wood test samples (at 12% moisture content) were used to calculate their average air-dried densities (D_{stick}). The dynamic elastic modulus was determined using the natural frequency of vibration along the fibre direction. A detailed description of this procedure was given by Ilic.[5]

Dimensions and masses of the SilviScan-2 test samples were used to calculate their average air-dried densities (D_{strip}), and MFA was estimated on SilviScan-2 using scanning x-ray diffractometry.[2-4] The experimental layout for scanning x-ray diffractometry of wood on SilviScan-2 is illustrated in Fig. 1. Schimleck et al.[6] found that the relation between laboratory-determined MFA and NIR fitted MFA was not linear for *E. delegatensis*. A simple transformation (100/MFA) was used to transform the data, giving an improved calibration. 100/MFA was calculated using the equation

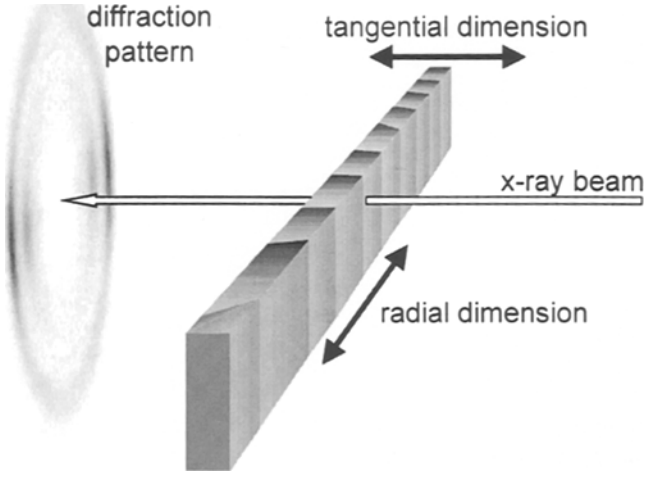

Fig. 1. Experimental arrangement for microfibril angle (MFA) measurement on SilviScan-2. Typical sample dimensions in this study were 2 mm (tangential), 7 mm (longitudinal), and 20 mm (radial). Samples were cut to maintain growth rings approximately parallel to the X-ray beam

$$100/\mathrm{MFA} = (1/\mathrm{MFA}) \times 100 \quad (1)$$

The specific longitudinal modulus of elasticity (specific E_L) was calculated using the equation

$$\text{Specific } E_L = E_L / D_{stick} \quad (2)$$

The E_L was also estimated based on SilviScan-2 data and the density of the stick[4] and is designated as $E_{L(SS)}$.

NIR spectroscopy

The NIR diffuse reflectance spectra were obtained from the radial/longitudinal face of each sample using a NIR Systems model 5000 scanning spectrophotometer. Samples were held in a custom-made holder. A 5 × 20 mm mask was used to ensure that a constant area was tested. The spectra were collected at 2-nm intervals over the wavelength range 1100–2500 nm. The instrument reference was a ceramic standard. Fifty scans were accumulated for each sample and the results averaged. One spectrum was obtained per sample. Experiments were conducted that demonstrated that the 2-mm strips could be considered to be infinitely thick for the power output of the NIR instrument used in this study.

The spectra were converted to the second derivative mode[8] for the development of calibrations using the instrument's NSAS software. A segment width of 10 nm and a gap width of 20 nm were used for the conversion.

Calibration

Calibrations were developed using partial least squares (PLS) regression. PLS regression is a data decomposition technique that extracts the systematic variation that exists in a single data set (X). It is possible to extract a few factors that explain most of the variation from NIR spectra because bands in NIR spectra display a large degree of intercorrelation.

The PLS regression involves simultaneous and interdependent principal components analysis (PCA) decomposition of both matrix **X** and matrix **Y**. The **X** matrix consists of n objects (rows, tested samples) and p variables (columns, absorbances at wavelengths in the NIR spectra); it is an $n \times p$ matrix. The **Y** matrix consists of n objects (defined as above) and q variables (in this study D_{stick}, D_{strip}, MFA, 100/MFA, E_L, specific E_L, and $E_{L(SS)}$ data); it is an $n \times q$ matrix. PLS uses the y-data structure (y-variance) to guide the decomposition of the **X** matrix.[9] Calibrations were developed using NSAS software (version 3.52). Calibrations were developed with four cross-validation segments and a maximum of ten factors. The selection of how many factors to use is important, and for all calibrations the final number of factors used was recommended by the software.[10]

Calibrations were developed using approximately two-thirds (n = 70) of the available samples, whereas the remaining one-third (n = 34) were used to test the predictive performance of the calibrations. Samples were selected at random for each set. A summary of wood properties for each set is given in Table 1.

Table 1. Range of wood properties for calibration and prediction sets

Wood property	Calibration set			Prediction set		
	Minimum	Maximum	Average	Minimum	Maximum	Average
$Density_{stick}$ (kg/m^3)	332.0	505.0	411.0	341.0	502.0	419.7
$Density_{strip}$ (kg/m^3)	305.1	540.4	423.0	324.0	524.9	427.4
MFA (degrees)	11.3	28.1	16.5	10.7	25.1	15.8
100/MFA (degrees^{-1})	3.6	8.8	6.4	4.0	9.4	6.6
E_L (GPa)	5.6	15.8	10.5	6.7	14.3	10.6
Specific E_L (MPa m^3/kg)	15.0	32.0	25.5	17.0	32.0	25.3
$E_{L(ss)}$ (GPa)	5.2	15.0	10.3	6.0	14.9	10.8

MFA, microfibril angle; E_L, longitudinal modulus of elasticity; $E_{L(ss)}$, longitudinal modulus of elasticity based on SilviScan-2 data

Calibration statistics

In this study the measure of how well a calibration fits the data is the standard error of calibration (SEC),[10–12] which is given by:

$$SEC = \sqrt{\frac{\sum_{i=1}^{NC}(\hat{y}_i - y_i)^2}{(NC - k - 1)}} \quad (3)$$

where $\hat{y}_i$ is the value of the constituent of interest for validation sample i estimated using the calibration; y_i is the known value of the constituent of interest of sample i; NC is the number of samples used to develop the calibration; and k is the number of factors used to develop the calibration.

In this study, a measure of how well the calibration predicts the constituent of interest for a set of unknown samples that are different from the calibration test set is given by the standard error of prediction (SEP).[10–12]

$$SEP = \sqrt{\frac{\sum_{i=1}^{NP}(\hat{y}_i - y_i)^2}{(NP - 1)}} \quad (4)$$

where $\hat{y}_i$ is the value of the constituent of interest for sample i predicted by the calibration; y_i is the known value of the constituent of interest for sample i; and NP is the number of samples in the prediction set.

Results and discussion

NIR calibrations for *P. radiata* solid-wood properties

Calibrations developed for each *P. radiata* solid-wood property are given in Table 2. The relations were good in all cases, with coefficients of determination (R^2) ranging from 0.68 for 100/MFA to 0.94 for $density_{strip}$. SEC and SEP results (note that the SEP was determined using the prediction set) for each calibration were similar for each property. The similar standard errors indicate that calibrations based on the NIR spectra of *P. radiata* solid-wood samples can be used to predict wood properties of a separate set.

The calibrations developed for $density_{strip}$ and $density_{stick}$ had calibration statistics that were quite different, but it should be noted that the $density_{stick}$ calibration was developed with five fewer factors. If the $density_{strip}$ calibration were developed using two factors, the R^2 (0.79) and SEC (21.68) were still superior. Plots of laboratory-determined density versus NIR fitted density for both the stick and strip calibrations are given in Figs. 2 and 3, respectively. NIR spectra collected from the surface of each strip were used to

Table 2. Summary statistics of calibrations developed for *Pinus radiata* solid-wood properties

Wood property	No. of factors	R^2	SEC	SEP
$Density_{stick}$ (kg/m^3)	2	0.69	22.85	21.80
$Density_{strip}$ (kg/m^3)	7	0.94	12.51	17.30
MFA (degrees)	3	0.78	1.91	2.11
100/MFA (degrees^{-1})	2	0.68	0.78	0.81
E_L (GPa)*	2	0.82	1.01	1.08
Specific E_L (MPa m^3/kg)[a]	5	0.88	1.46	1.82
$E_{L(ss)}$ (GPa)	2	0.83	0.92	0.91

Note: calibrations were developed using 69 samples
SEC, standard error of calibration; SEP, standard error of prediction

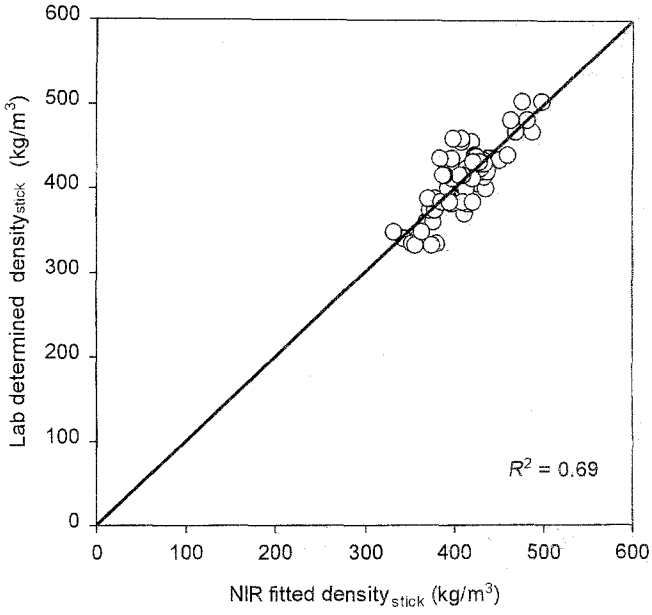

Fig. 2. Plot of laboratory-determined $density_{stick}$ versus near-infrared (NIR) fitted $density_{stick}$

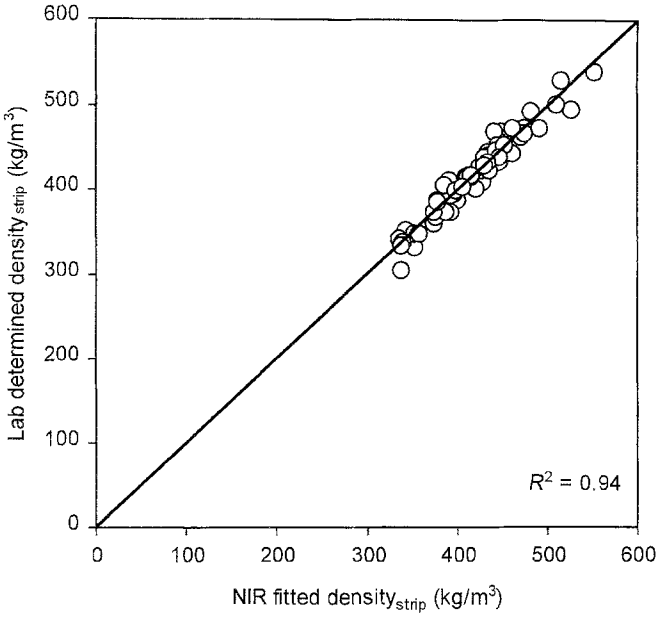

Fig. 3. Plot of laboratory-determined density$_{strip}$ versus NIR fitted density$_{strip}$

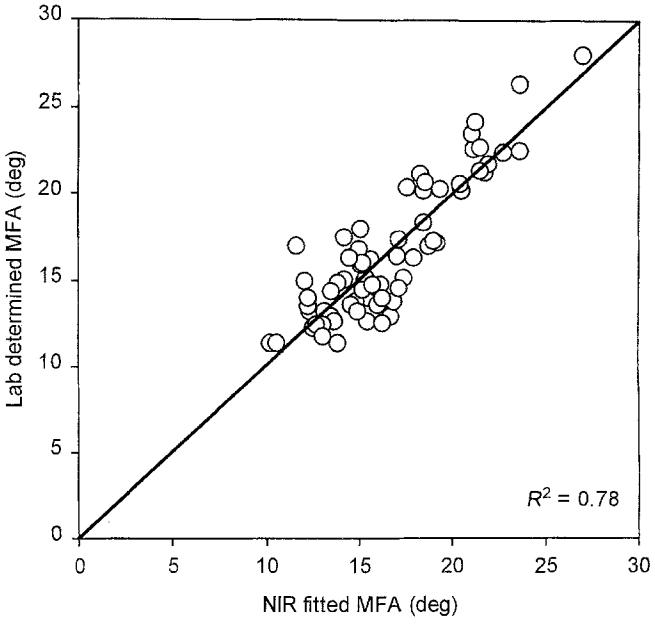

Fig. 5. Plot of laboratory-determined MFA versus NIR fitted MFA

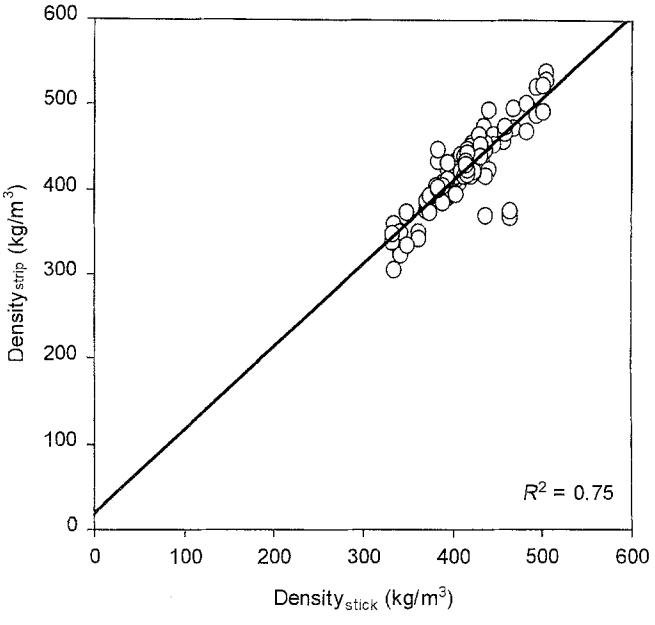

Fig. 4. Plot of density$_{strip}$ versus density$_{stick}$

develop the density$_{stick}$ calibration. Consequently, the density$_{stick}$ calibration depends on the relation between density$_{stick}$ and density$_{strip}$. A poor relation between the two gives a poor NIR calibration for density$_{stick}$. The relation between the two was good (R^2 = 0.75) (Fig. 4) but not as strong as expected based on the strong relation reported (R^2 = 0.98) for the *E. delegatensis* samples studied previously.[4,6] Three samples had strip and stick densities that were quite different, and their exclusion improved the R^2 to 0.88. Two of these samples were part of the prediction set and were detected as outliers (based on their large residuals, note that the residual = NIR fitted value − laboratory-determined value) and excluded when the density$_{stick}$ and specific E_L calibrations were applied to the prediction set. A small bias exists because the strips that were removed from the sticks generally had higher densities.

It was observed that *P. radiata* samples of different densities demonstrated considerable baseline shifts; NIR spectra of high-density samples were shifted upward relative to spectra of low-density samples. When a calibration for density (stick or strip) was developed, it was strongly influenced by these baseline shifts.

The calibration developed for MFA (Fig. 5) had an R^2 of 0.78. Generally MFA was well fitted, and most of the samples had residuals of less than 3°. One sample was observed to have a very large residual (−5.4°). The calibration developed for MFA had a higher R^2 than the 100/MFA calibration. In contrast, Schimleck et al.[6] reported that the 100/MFA calibration was more successful for *E. delegatensis*. They observed that the distribution of MFAs in the *E. delegatensis* sample set was skewed, with most of the samples having MFAs of less than 12°, and they suspected that poor estimates when the MFA was greater than 17° was caused by the skewed distribution. The *P. radiata* sample set, in comparison, had a more even distribution of MFAs. The good calibration statistics obtained for MFA may be due to the systematic within-tree variation in a range of associated properties, such as cellulose content, that would be expected to exist within this sample set.

The calibrations developed for E_L and specific E_L had coefficients of determination of 0.82 and 0.88, respectively. A plot of laboratory-determined E_L versus NIR fitted E_L is given in Fig. 6. The E_L was well fitted over the range of the calibration (5.6–15.8 GPa). Two samples had residuals of more than 2 GPa. An important factor in the success of the E_L and specific E_L calibrations was the baseline shift that

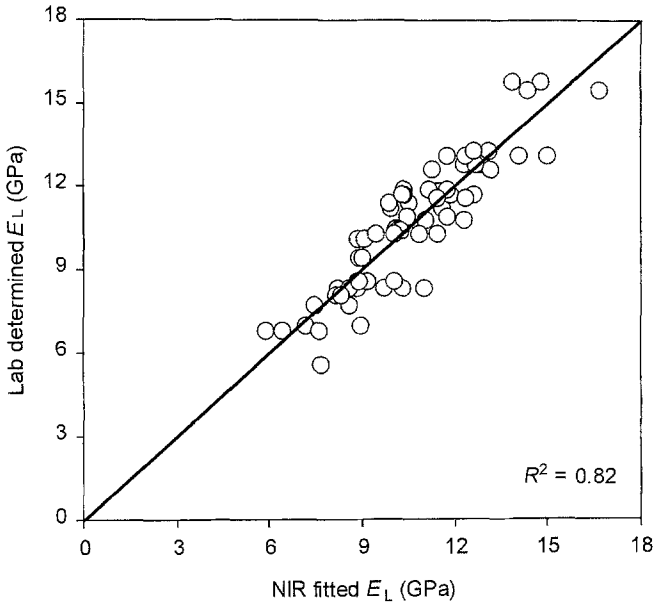

Fig. 6. Plot of laboratory-determined longitudinal modulus of elasticity (E_L) versus NIR fitted E_L

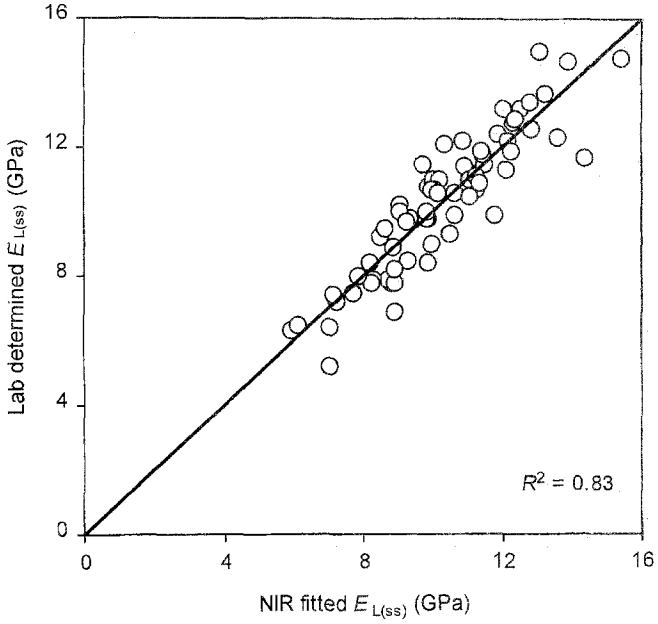

Fig. 8. Plot of laboratory-determined E_L based on SilviScan-2 data and the density of the stick ($E_{L(ss)}$) versus NIRS fitted $E_{L(ss)}$

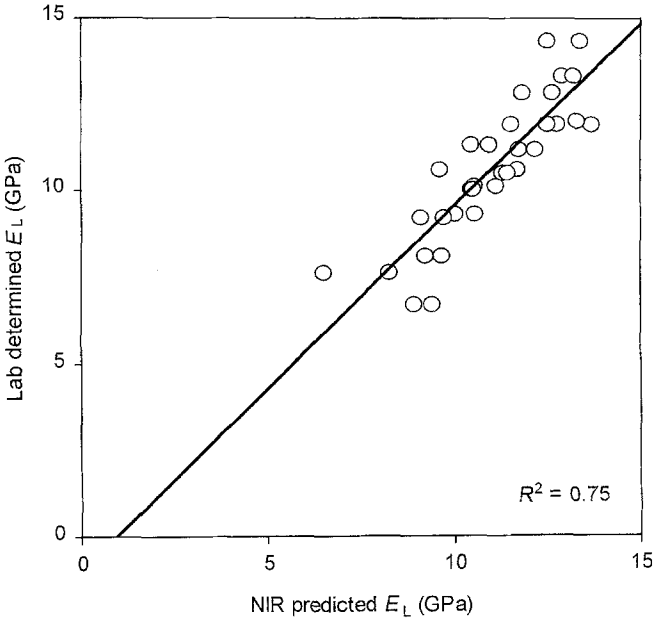

Fig. 7. Plot of laboratory-determined E_L versus NIR predicted E_L

had been observed for samples of differing density. The E_L calibration performed well for predicting the separate test set (Fig. 7). A small bias exists (0.398) because the calibration tended to overestimate E_L. If the two samples that had the largest residuals were removed, the bias would be almost nonexistent.

The calibration developed for $E_{L(SS)}$ (Fig. 8) was similar to the calibration developed for E_L. Two samples had residuals of more than 2 GPa, the largest being 2.7 GPa. The $E_{L(SS)}$ calibration had a lower SEC than the E_L calibration, indicating that the residuals for the $E_{L(SS)}$ calibration were smaller. This finding suggests that an NIR instrument could be calibrated to estimate the E_L of increment cores, based on data collected by SilviScan-2. Further experiments have been conducted at our laboratory and will be reported later. Significantly, $E_{L(SS)}$ was observed to be strongly correlated with E_L (R^2 = 0.86). The relation was not as strong as that found for *E. delegatensis* (R^2 = 0.96).[4]

Calibrations reported in this study demonstrate that properties of *P. radiata* clear wood can be estimated by NIR spectroscopy. An important aspect in the success of this work was that the strips used for NIR analysis were representative of the sticks from which they were removed. If the methods described in this paper were applied to larger samples (i.e., boards), it is probable that the strips removed for analysis would poorly represent the sample and the calibrations would suffer.

The NIR spectra were measured from the surface of wooden strips that can easily be prepared from increment core samples, facilitating the nondestructive sampling of standing trees. For nondestructive sampling to be successful, the core must represent the whole tree. Studies are being conducted that investigate the relations between wood properties estimated by NIR spectroscopy on core samples and whole trees.

Conclusions

The use of calibrated NIR spectroscopy for predicting a range of *Pinus radiata* clear wood properties was investigated. NIR spectra were obtained from the radial/longitudinal face of each sample and were used to generate calibrations for a number of solid wood properties including

$density_{stick}$, $density_{strip}$, MFA, 100/MFA, E_L, and specific E_L determined using SilviScan-2 data. The relations between laboratory-determined data and NIR fitted data were good in all cases, indicating that useful calibrations for a number of important solid wood samples can be developed using NIR spectroscopy. The calibrations were also used successfully to predict wood properties of samples in a separate set. These results and others widely reported in the literature indicate that NIR spectroscopy can be calibrated for predicting a number of wood properties, making NIR spectroscopy an important tool for cost-effective evaluation of wood properties in tree breeding and resource evaluation studies.

Acknowledgments The authors thank Sharee Stringer and Jenny Carr for their technical assistance.

References

1. Evans R (1994) Rapid measurement of the transverse dimensions of tracheids in radial wood sections from *Pinus radiata*. Holzforschung 48:168–172
2. Evans R (1997) Rapid scanning of microfibril angle in increment cores by x-ray diffractometry. In: Butterfield BG (ed) Microfibril angle in wood. University of Canterbury, Christchurch, pp 116–139
3. Evans R (1999) A variance approach to the x-ray diffractometric estimation of microfibril angle in wood. Appita J 52:283–289, 294
4. Evans R, Ilic J (2001) Rapid prediction of wood stiffness from microfibril angle and density. For Prod J 51(3):53–57
5. Ilic J (2001) Variation of the dynamic elastic modulus and wave velocity in the fibre direction with other properties during the drying of *Eucalyptus regnans* F. Muell. Wood Sci Technol 35(1/2):157–166
6. Schimleck LR, Evans R, Ilic J (2001) Estimation of *Eucalyptus delegatensis* wood properties by near infrared spectroscopy. Can J For Res 31(10):1671–1675
7. Evans R, Ilic J, Matheson AC (2000) Rapid estimation of solid wood stiffness using SilviScan. In: Schimleck LR, Blakemore PA (eds) Proceedings of the 26th forest products research conference. CSIRO Forestry and Forest Products, Clayton, pp 49–50
8. Shenk JS, Workman JJ Jr, Westerhaus MO (1992) Application of NIR spectroscopy to agricultural products. In: Burns DA, Ciurczak EW (eds) Handbook of near-infrared analysis. Marcel Dekker, New York, pp 385–386
9. Esbensen K, Schönkopf S, Midtgaard T (1994) Multivariate analysis in practice. Camo AS, Trondheim
10. Anonymous (1990) Manual for NIR spectral analysis software. NIRSystems, Silver Spring, MD, USA
11. Miller CE (1989) Analysis of synthetic polymers by near-infrared spectroscopy. PhD thesis, University of Washington, pp 55–56
12. Workman JJ Jr (1992) NIR spectroscopy calibration basics. In: Burns DA, Ciurczak EW (eds) Handbook of near-infrared analysis. Marcel Dekker, New York, pp 274–276